We are IntechOpen, the world's leading publisher of Open Access books
Built by scientists, for scientists

4,800
Open access books available

122,000
International authors and editors

135M
Downloads

Our authors are among the

154
Countries delivered to

TOP 1%
most cited scientists

12.2%
Contributors from top 500 universities

CLARIVATE ANALYTICS
BOOK CITATION INDEX
INDEXED

WEB OF SCIENCE™

Selection of our books indexed in the Book Citation Index in Web of Science™ Core Collection (BKCI)

Interested in publishing with us?
Contact book.department@intechopen.com

Numbers displayed above are based on latest data collected.
For more information visit www.intechopen.com

Chapter 3

Materials Used in High-Speed Electrical Machines

Flyur R. Ismagilov, Viacheslav Ye. Vavilov and Valentina V. Ayguzina

Additional information is available at the end of the chapter

http://dx.doi.org/10.5772/intechopen.79627

Abstract

The high-speed electrical machines are widely used in different industries, such as machine tools, aerospace engineering, autonomous power engineering, etc. This chapter devoted to materials used in high-speed electrical machines with high-coercitivity permanent magnets (HCPMs). It is considered to be materials of rotor sleeve, shaft, stator magnetic core, and permanent magnet. Material selection methods are presented. In addition, mechanical strength calculation of the rotor sleeve is shown. The obtained results can be used in the design of high-speed electrical machines with high-coercivity permanent magnets and in their future development.

Keywords: high-speed electrical machine, high-coercivity permanent magnets, rotor magnetic system, amorphous magnetic material, eddy-current losses, windage losses

1. Introduction

Mass and size and energy parameters, reliability, and efficiency of high-speed and ultra-high-speed electric machines (EMs) are determined and ensured by the properties of the materials used in them. Therefore, special attention should be given to the selection of materials with the necessary properties in the high-speed EM design process.

Materials used in the static components of high-speed EM (housing, bearing shields, cooling elements, etc.) are no different from the materials of the traditional industrial EMs. But materials used in rotating parts (shaft, rotor shroud, rotor back, etc.) of high-speed EMs with high-coercivity permanent magnet (HCPM) should have increased strength characteristics, from which the EM operating conditions, limiting rotational speed, and power are determined. For example, the air gap value is determined by the rotor sleeve strength of the high-speed EM

IntechOpen

© 2018 The Author(s). Licensee IntechOpen. This chapter is distributed under the terms of the Creative Commons Attribution License (http://creativecommons.org/licenses/by/3.0), which permits unrestricted use, distribution, and reproduction in any medium, provided the original work is properly cited. CC BY

with the HCPM. Therefore, materials used in rotating parts of the high-speed EM with HCPM are discussed in the following sections in more detail.

2. Rotor sleeve materials of the high-speed EM

At high rotor rotational speeds, the centrifugal forces acting on the HCPM tend to tear them away from the shaft. To counteract these forces and to ensure the rotor mechanical strength, the rotor sleeve is used. The rotor sleeve is installed over the HCPM with a certain shrink fit and can be made as a single nonmagnetic sleeve or wound on the HCPM with a composite material filament glued with epoxy resin. **Figure 1a** shows a rotor with a rotor sleeve made of composite material, and **Figure 1b** shows the rotor sleeve made of composite material. Properties of composite materials used in the rotor sleeve [1] are presented in **Table 1**.

The use of composite materials in the high-speed EMs is more technological than the use of solid non-magnetic sleeves, but this technology requires specialized winding equipment, which limits its wide application. Therefore, in a number of cases, one-piece sleeves are used that are installed with a certain shrink fit on the rotor. Titanium or Inconel 718 is used as a material of the rotor sleeve. **Table 2** shows the main characteristics of these materials.

In addition, to select the rotor sleeve material, it is necessary to take into account that the outer surface of the rotor sleeve determines the friction coefficient, which affects the friction losses. To minimize these losses, special antifriction coatings can be used of which the application increases the efficiency of high-speed EM to 0.5% according to [2].

In the rotor sleeve design, it is necessary to take into account the thermal and mechanical extensions of the rotor sleeve during operation. These extensions in some cases can reach 0.3–0.5 mm. If the air gap is incorrectly selected, the expansion can lead to a mechanical contact between the stator and the rotor, which is unacceptable. That is, this criterion also plays an important role in the material selection of the rotor sleeve.

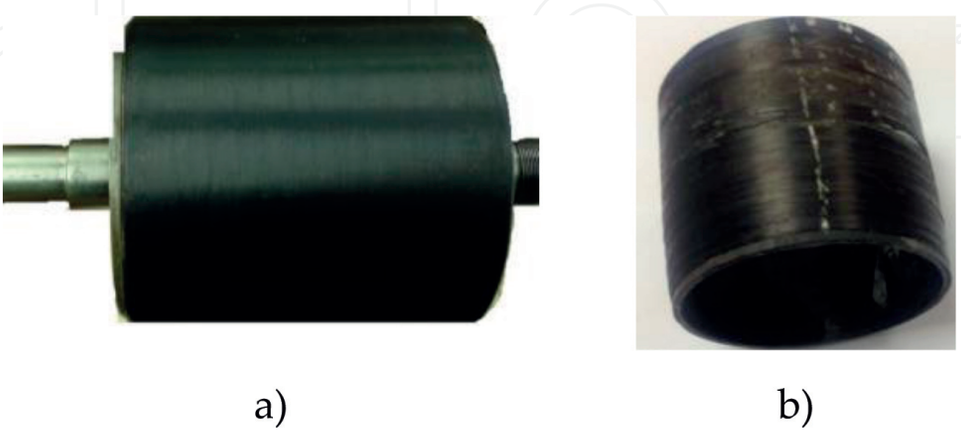

Figure 1. Rotor (a) with a rotor sleeve made of composite material (b).

Property	GFRP DW 210	AFRP DW 152	CFRP DW 231	CFRP DW260
Tensile strength (MPa)	1440	1880	2420	2420
Density (kg/m^3)	2100	1330	1520	1520
Maximum operating temperature (°C)	<110	<140	<140	>300
Thermal expansion coefficient	7	0.2	0.2	0.2

Table 1. Properties of composite materials used in the rotor sleeve [1].

Characteristics	Titanium	Inconel 718
Tensile strength (MPa)	1191–1230 (depending on the treatment type)	1443–1553 (depending on the treatment type)
Density (kg/m^3)	4600	8190
Thermal expansion coefficient	7.7–10.4 (depending on the treatment type)	9.5–20.5 (depending on the treatment type)

Table 2. The main characteristics of Titanium and Inconel 718.

It is also important to notice that almost all the materials that are used in the rotor sleeve have electrical conductivity, which leads to eddy currents and heating of the rotor sleeve and HCPM. Therefore, the rotor sleeve should have a minimum electrical conductivity.

2.1. Mechanical strength calculation of the rotor sleeve

In [3], equations for the rotor sleeve thickness calculations are given. These equations do not take into account thermal expansions of the rotor sleeve and shrink fit. Therefore, they are approximate and do not satisfy the specified design accuracy. It seems expedient to consider in more detail the design process of the rotor sleeve of high-speed EM.

In the rotor sleeve calculation, the nominal and maximum rotational speeds are assumed to be set. The material properties, the shrink fit value, and the main rotor geometric dimensions are considered to be known.

It is important to notice that the selection of the rotor sleeve thickness is an important component of the high-speed EM design process. In **Figure 2**, the stress dependencies of the HCPM and the rotor sleeve made of titanium and Inconel 718 obtained in [4] for the EM with a rotational speed of 30,000 rpm are given as an example. It can be seen that an increase in the rotor sleeve shrink fit by 100% leads to a reduction in mechanical stresses in the HCPM by 260% and an increase in mechanical stresses in the rotor sleeve by 60%. The shrink fit value should be selected that the maximum stresses in the rotor sleeve are below the maximum permissible stresses of the material used by 20–30%, and stresses in the HCPM are below the maximum permissible stresses by 20–30%.

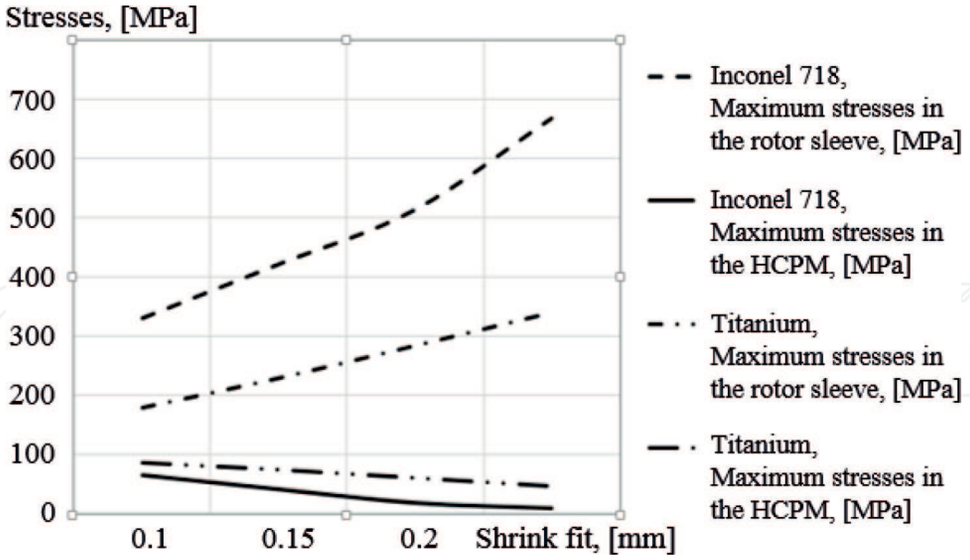

Figure 2. The stress dependences of the HCPM and the rotor sleeve made of titanium and Inconel 718 [4].

The centrifugal forces of the rotor sleeve are determined by the following:

$$F_{\mathrm{r.s}} = 11.1 m_{\mathrm{r.s}} r_{\mathrm{r}} \left(\frac{n}{1000}\right)^2, \tag{1}$$

where $F_{\mathrm{r.s}}$ is the centrifugal force of the rotor sleeve; $m_{\mathrm{r.s}}$ is the rotor sleeve mass; n is a rotational speed; and r_{r} is a rotor radius.

The inertia radius is determined by the known equation: $r_{\mathrm{r}} = \frac{2}{3} r_2 \frac{1+\alpha_{\mathrm{r}}+\alpha^2{}_{\mathrm{r}}}{1+\alpha_{\mathrm{r}}}$, where $\alpha_{\mathrm{r}} = \frac{r_1}{r_2}$ is a rotor radius ratio.

The centrifugal force of the rotor: $F_{\mathrm{r}} = \frac{2,93}{8} \rho_{\mathrm{r}} l r_2{}^3 \left(1 - \alpha^3{}_{\mathrm{r}}\right) \left(\frac{n}{1000}\right)^2$, where $\rho_{\mathrm{r}} = \frac{\rho_1+\rho_2}{2}$ is the average density of rotor materials, ρ_1 and ρ_2 are, respectively, the density of the HCPM and shaft material.

The preliminary thickness of the rotor sleeve is determined without taking into account the rotor sleeve mass (**Figure 3**):

$$b = \frac{\Omega^2 \rho_1 (r_1 + r_2)\left(D^2{}_4 - D^2{}_3\right)}{16\sigma_{\mathrm{M}}} k_\sigma, \tag{2}$$

where Ω is a rotor rotational speed, (rad/s); σ_{M} is the tensile strength of the rotor sleeve material; D_3, D_4 are, respectively, the inner and outer HCPM diameters; k_σ is the rotor sleeve safety factor, which is taken in the range from 1.2 to 1.5.

Radial sectional area of the rotor sleeve: $S_{\mathrm{r.s}} = \frac{\pi\left(8 r_2 b + 4 b^2\right)}{4}$.

Tangential stresses on the inner surface of the rotor sleeve: $\sigma = \frac{\eta_1 F_{\mathrm{s.r}}}{2\pi S_6} \left(\frac{n}{1000}\right)^2$, where η_1 is the coefficient of tangential forces on the inner surface of the rotor sleeve, which is determined from **Figure 4**.

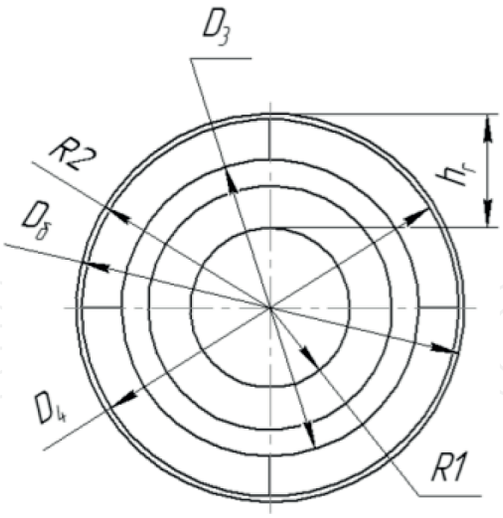

Figure 3. Calculation scheme of the high-speed EM.

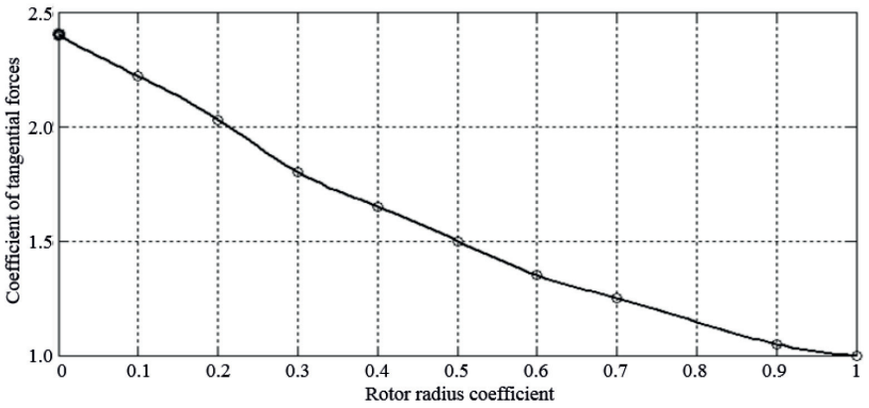

Figure 4. Dependence of the coefficient of tangential forces on the rotor radius coefficient.

Tangential stresses on the outer surface of the rotor sleeve: $\sigma' = \frac{\eta_2 F_{s.r}}{2\pi S_{r.s}} \left(\frac{n}{1000}\right)^2$, where η_2 is the coefficient of tangential forces on the outer surface of the rotor sleeve.

Then calculations are carried out according to the calculation scheme shown in **Figure 3** and the method presented in [5].

Stresses in the rotor sleeve should be less than the tensile strength of the rotor sleeve material, and the rotor sleeve should create a pressure for the HCPM [5]:

$$p_N = p_p + p_t - p_z > 0, \quad k_\sigma(\sigma_p + \sigma_t + \sigma_z) < \sigma_M; \tag{3}$$

where p_N is the residual rotor sleeve pressure on the permanent magnets; p_p, σ_p are, respectively, the pressure and mechanical stress produced by the rotor sleeve preload; p_t, σ_t are, respectively, the pressure and mechanical stress produced by the thermal expansion of the rotor and permanent magnets; p_z, σ_z are, respectively, the pressure and mechanical stress produced by centrifugal forces.

Pressure and mechanical stress produced by the preload are defined by [5]:

$$\sigma_{\mathrm{p}} = \frac{2\Delta D_{\mathrm{r.s}}}{D} E_{\mathrm{r.s}}, \quad p_{\mathrm{p}} = \sigma_{\mathrm{p}} \left[\frac{r_1^2}{r_1^2 - r_2^2} \left(1 + \frac{r_2^2}{r_3^2} \right) \right]^{-1}; \tag{4}$$

where $\Delta D_{\mathrm{r.s}}$ is the rotor sleeve preload; $r_1 = \frac{D_{\mathrm{r.s}}}{2}$; $r_2 = \frac{D}{2}$; $r_3 = \frac{D_{\mathrm{m}}}{2}$.

The pressure and mechanical stress produced by the rotor thermal expansion are determined [5]:

$$\sigma_{\mathrm{t}} = \frac{2\Delta D_{\mathrm{T}}}{D} E_{\mathrm{r.s}}, \quad p_{\mathrm{t}} = \sigma_{\mathrm{t}} \frac{b}{R_{\mathrm{r.s}}}; \tag{5}$$

where $\Delta D_{\mathrm{T}} = \alpha_{\mathrm{Bt}} D(T_2 - T_1)$ is the linear expansion of permanent magnets under the temperature; α_{Bt} is the linear expansion coefficient of permanent magnets; T_2, T_1 are the temperatures of permanent magnets at the ultra-high-speed electrical machine (UHSEM) operation beginning and the steady UHSEM temperature, respectively.

The pressure and the mechanical stress produced by centrifugal forces [5]:

$$\sigma_{\mathrm{z}} = \Omega^2 r_3^2 \rho_{\mathrm{r.s}}^2, \quad p_{\mathrm{z}} = \rho_{\mathrm{r.s}} \Omega^2 r_3 b; \tag{6}$$

where $\rho_{\mathrm{r.s}}$ is the density of the bandage material.

After determining the pressure and mechanical stress in the bandage, checking its mechanical strength is performed according to Eq. [5]:

$$p_{\mathrm{N}} = p_{\mathrm{p}} + p_{\mathrm{t}} - p_{\mathrm{z}} > 0, \quad k_{\sigma}(\sigma_{\mathrm{p}} + \sigma_{\mathrm{t}} + \sigma_{\mathrm{z}}) < \sigma_{\mathrm{M}}. \tag{7}$$

3. Shaft materials of the high-speed EMs

The shaft of the high-speed EM provides the necessary rotor stiffness, its mechanical strength, and magnetic properties. The magnetic field of the HCPM should not be closed through bearings to avoid the occurrence of bearing currents. Therefore, it is advisable to use a prefabricated shaft with a back made of magnetic material and a shaft made of a nonmagnetic material. The use of fully nonmagnetic shafts is recommended only for the combined and Halbach magnetic systems. In all other cases, the use of a nonmagnetic shaft will reduce the magnetic flux density in the air gap by 15–25%. For fully magnetic shafts, it is necessary to insulate the bearings. For the nonmagnetic part of the shaft, either titanium or Inconel 718 is usually used.

4. Stator magnetic core materials of the high-speed EMs

Prospects for the use of a particular material of the stator magnetic core in high-speed EMs are determined by the minimum losses, mass and size parameters of the stator magnetic core and EM, maximum EM power and maximum magnetic flux density in the air gap, cost of the stator

magnetic core, and manufacturability. Thus, the selection task of the optimal stator magnetic core material is the task of multicriteria optimization. As a selection criterion, the mass and size EM parameters, magnetic flux density, efficiency, manufacturability, and cost of the of the stator magnetic core are used. Since each of these criteria can be represented as a function of magnetic flux density in the stator back and teeth, it is possible to formulate a mathematical function of the stator magnetic core material selection. By using this function for the specified maximum values of the specific losses in the stator back and teeth, the cost of the stator magnetic core, production technology, and effectiveness of a given material can be numerically justified. Taking into account that this is an optimization task, it should be solved after preliminary EM calculations, which will determine the geometric dimensions of the stator magnetic core and electromagnetic loads (linear current load, magnetic flux density in the air gap, etc.). All the aforementioned criteria should be presented as functions of the steel properties. For example, such dependence for magnetic flux density in the air gap is determined from the magnetic circuit calculation:

$$F_{\mathrm{M}} = 2F_{\delta} + 2F_{\mathrm{z}} + F_{\mathrm{j}} + F_{r}, \tag{8}$$

where $F_{\mathrm{M}} = H_{\mathrm{M}} l_{\mathrm{M}}$ is the magnetomotive force (MMF) of the HCPM; $H_{\mathrm{M}} l_{\mathrm{M}}$ is a product of the magnetic field strength in the HCPM by the length of the average magnetic line in the HCPM; F_{δ} is the MMF of the air gap; F_{j} is the MMF of the stator back; F_{z} is the MMF of the stator teeth; and F_{r} is the MMF of the rotor back and shaft.

Eq. (15) is represented in the form of the MMF dependences on the magnetic flux density and the magnetic field strength:

$$F_{\mathrm{M}} = 2B_{\delta} k_{\delta} \delta + 2H_{\mathrm{z}} h_{z} + H_{\mathrm{j}} h_{\mathrm{j}} + H_{\mathrm{r}} h_{\mathrm{r}}, \tag{9}$$

where B_{δ} is a magnetic flux density in the air gap; δ is an air gap; $H_{\mathrm{z}} = B_{\mathrm{z}}/\mu_{\mathrm{s}}\mu_{0}$ is the magnetic field strength in the stator teeth; $H_{\mathrm{j}} = B_{\mathrm{j}}/\mu_{\mathrm{s}}\mu_{0}$ is the magnetic field strength in the stator back; $H_{\mathrm{r}} = B_{\mathrm{r}}/\mu_{\mathrm{r}}\mu_{0}$ is the magnetic field strength in the rotor back; $h_{z}, h_{\mathrm{j}}, h_{\mathrm{r}}$ are the height of the stator tooth, stator back, and rotor back, respectively; and k_{δ} is an air gap coefficient.

One of the features of the EM with HCPM is that it is necessary to perform a check of the magnetic circuit saturation in the idle mode, since under load, the armature reaction magnetic field and the HCPM heating reduce the magnetic flux density in the air gap but do not demagnetize the HCPM. Therefore, in selection of the stator magnetic core material of the high-speed EM, the MMF of the HCPM can be considered as constant. The dependence of the magnetic flux density in the air gap can be represented as a function of magnetic flux density in the stator back and in the stator teeth according to Eq. (16).

The mass of the stator magnetic core is determined by the magnetic flux density in the stator back and teeth, as well as the density of the stator magnetic core material, and can be represented as a function of these parameters. The efficiency is determined by the specific losses of the stator magnetic core material, which can be approximated as a function of frequency, empirical coefficients, and magnetic flux density in the stator back and teeth. The cost of the stator magnetic core is determined by the total mass of the material used in its manufacture (taking into account the

mass of waste during stamping or cutting), as well as the manufacture complexity. The task of the stator magnetic core material selection can be represented as a mathematical function:

$$\begin{cases} B_\delta(B_z, B_j) \rightarrow \max \\ M_M(B_z, B_j) \rightarrow \min \\ \eta(B_z, B_j) \rightarrow \max \\ C(B_z, B_j) \rightarrow \min \\ M_{waste}(B_z, B_j) \rightarrow \min \end{cases}, \tag{10}$$

where $B_\delta(B_z, B_j)$ is a magnetic flux density in the air gap; $M_M(B_z, B_j)$ is the EM mass; $\eta(B_z, B_j)$ is the EM efficiency; $C(B_z, B_j)$ is the cost of the stator magnetic core; and $M_{waste}(B_z, B_j)$ is a mass of the waste.

Thus, after determining the maximum permissible values of the magnetic flux density for the stator teeth and back for a specific stator magnetic core material and approximating the specific loss function, the value of each criterion included in Eq. (17) can be determined. Then, a comparative multicriteria analysis of the material expediency and the optimal selection of the stator magnetic core material can be made.

To reduce the number of compared criteria, Eq. (17) can be reduced to a task with one criterion by determining the weight of each function in Eq. (17):

$$f(B_z, B_j) = \lambda_1 B_\delta(B_z, B_j) - \lambda_2 M_M(B_z, B_j) + \lambda_3 \eta(B_z, B_j) - \lambda_4 C(B_z, B_j) - \lambda_4 M_{waste}(B_z, B_j) \rightarrow \max, \tag{11}$$

where $\lambda_1 \ldots \lambda_5$ is, respectively, the weight of each criterion in the overall efficiency function of using a particular stator magnetic core material.

In conversion from the multicriteria comparison task to the function of one variable, which characterizes the effectiveness of the material application, it is necessary to replace the dimensional units in Eq. (17) by the relative units:

$$y^* = \frac{Y(B_z, B_s)}{Y_m(B_z, B_s)}, \tag{12}$$

where y^* is a criterion in relative units; $Y(B_z, B_s)$ is a criterion in dimensional units; and $Y_m(B_z, B_s)$ is a base value in dimensional units.

Since the efficiency of using a known electrotechnical steel or a precision soft magnetic alloy is determined, the base values are parameters in Eq. (18) at a saturation magnetic flux density for a given electrical steel or a precision soft magnetic alloy:

$$\begin{aligned} Ef(B_z, B_j) = &-\lambda_1 \frac{B_\delta(B_z, B_j)}{B_\delta(B_{zn}, B_{jn})} + \lambda_2 \frac{M_M(B_z, B_j)}{M_M(B_{zn}, B_{jn})} - \\ &-\lambda_3 \frac{\eta(B_z, B_j)}{\eta(B_{zn}, B_{jn})} + \lambda_4 \frac{C(B_z, B_j)}{C(B_{zn}, B_{jn})} + \lambda_4 \frac{M_{waste}(B_z, B_j)}{M_{waste}(B_{zn}, B_{jn})} \rightarrow \min, \end{aligned} \tag{13}$$

where $Ef(B_z, B_j)$ is the efficiency of stator material use.

Thus, the general condition for the stator magnetic core material selection can be formulated as follows. From two stator magnetic core materials, more effective is one with less $Ef\left(B_z, B_j\right)$ for the same $\lambda_1 \ldots \lambda_4$. For practical application of the proposed technique, different stator magnetic core material types of the high-speed EMs are considered.

4.1. Electrical steels and soft magnetic alloys

Figure 5 shows the dependences of the specific losses on frequency for various electrical steels. In the high-speed EM, silicon electrical steels are widely used. The main advantages of electrical steels are the simple production technology of the stator magnetic core of the high-speed EM. The disadvantage is a low-saturation magnetic flux density, which leads to an increase in the mass and size parameters of the EM. Higher saturation magnetic flux density has soft magnetic alloys based on cobalt or nickel, for example, VACOFLUX 50, VACOFLUX 48, VACODUR S Plus, VACODUR 50, VACODUR 49, VACOFLUX 18 HR, and VACOFLUX 17. The saturation magnetic flux density for these types of alloys varies from 2.14 to 2.35 T. **Figure 6** shows the magnetization curves for VACOFLUX 48 and VACODUR 49 alloys. The soft magnetic alloys with high saturation induction have significant specific losses that can be reduced by reducing the sheet thickness. In this case, even with a sheet thickness of 0.1 mm, it is inferior to electrical steels. In addition, soft magnetic alloys have a complex production technology and require special treatment. Therefore, these alloys predominantly find wide application in EM with magnetization frequencies below 400 Hz. At higher frequencies, the use of this alloy type requires justification.

4.2. Amorphous magnetic materials (AMMs)

AMM is a kind of alloy, which lacks the periodicity in the atom arrangement. AMMs are produced in the form of thin tape. The thickness of the tape is 25–30 μm.

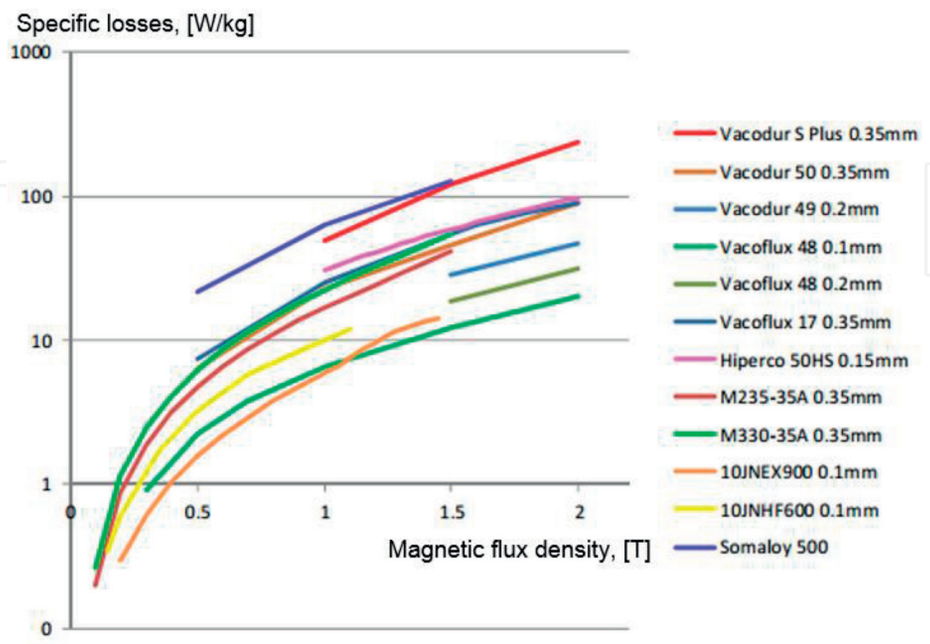

Figure 5. The dependences of the specific losses on frequency for various electrical steels.

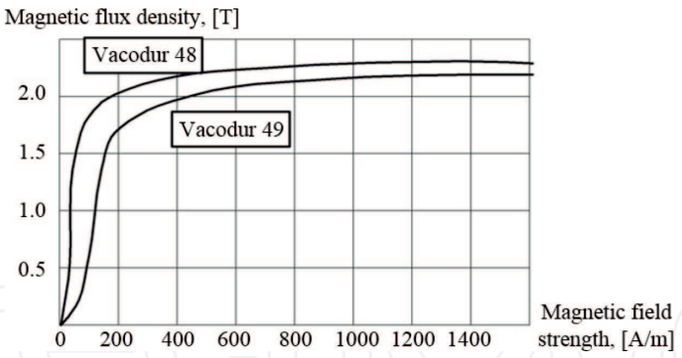

Figure 6. Magnetization curves for VACOFLUX 48 and VACODUR 49 alloys.

The AMM technology was developed in 1960 by a research group of the California Institute of Technology. In 1988, Hitachi Metals first developed a nanocrystalline alloy (metal glass).

The composition of the AMM includes two groups of elements: transition metals (Fe and Co) and amorphous elements (B, C, and Si). The amorphous alloy structure is obtained only at a certain cooling rate. In the AMM structure, there is no periodicity in the atom arrangement. Despite the fact that the AMM density is lower than the density of crystalline analogs, their strength is higher by 400–900% [6]. The higher strength is because the AMMs have no defects such as dislocations and grain boundaries inherent in the crystalline state. The presence of such defects greatly complicates the diffusion (penetration of atoms) through amorphous metallic layers.

The AMM advantages are high wear resistance, high corrosion resistance, high electrical resistivity (ϱ = 1–1.5 $\Omega \cdot mm^2$), low coercive force Hc (less than 8 A/m), high values of magnetic permeability (initial magnetic permeability μ_{in} is up to 8000, and maximum magnetic permeability μmax is up to 300,000–700,000), and low specific losses.

The AMM disadvantage is that it is produced in the form of a thin tape. And it is impossible to make a stator magnetic core by using traditional design technologies. Therefore, slotless stator magnetic core designs or designs with a large area and a small number of slots are used. In addition, AMMs has low saturation induction. For example, the maximum saturation induction value is 1.8 T for Metglas Alloy 2605CO.

Nevertheless, the development of the AMM production technologies makes it possible to talk about their prospects of using in the EM stator magnetic cores. For example, Hitachi has already created an induction motor with the energy efficiency class IE 4 with an AMM stator magnetic core. Radam and Celeroton also actively create the high-speed EMs with the AMM stator magnetic core.

The main AMM features are associated with several facts:

- The fill factor of the AMM stator magnetic core varies from 0.7 to 0.8 because in the AMM production, various defects are formed on the tape.
- AMM tape thickness does not exceed 25–30 μm; therefore, AMM magnetic cores are usually wound.

- AMM has a low saturation magnetic flux density, which usually varies from 1.3 to 1.6 T. For the cobalt-doped AMM, the magnetic flux density increases to 1.8 T. However, the specific losses also increase due to the increase in electrical conductivity.
- The AMM layers in the magnetic cores are not isolated from each other.

These features do not allow the use of known designs in the EMs with the AMM magnetic cores. Therefore, further, it seems appropriate to consider in more detail the AMM magnetic core designs and their technological approaches.

It is promising to use AMM in the high-speed EMs with a rotational speed of below 120,000 rpm and in the ultra-high-speed EMs with a rotational speed above 1,200,000 rpm. For the high magnetization reversal frequency, AMMs are practically the only correct technical solution. In micro-EM with rotational speeds above 700,000 rpm and magnetic flux density in the air gap of 0.2–0.25 T, the use of ferrites is effective, but a low saturation magnetic flux density is limited only by this narrow application field.

Due to the technological complexity of the AMM stator cores, several designs are used:

- EM with a tooth-coil stator magnetic core made of AMM, which forms from U-shaped AMM cores (**Figures 7–9**). The disadvantage of these cores is the technological complexity, and they are mainly performed with a large area and a small number of slots. The problem solution of a small number of slots can be the use of a sectional design of the EM with a stator magnetic core made of AMM (**Figure 10**).
- EM with prefabricated designs of the AMM stator magnetic cores. These designs are characterized by the fact that the magnetic core parts are made separately from simple geometric shapes, after which they are assembled. This technology is of particular interest for axial EM. Various designs of these magnetic cores are shown in **Figure 11**.

In addition, individual geometric figures can be performed not wound but by typing from plates. Further, these sets are inserted into the stator. For example, in [8], a radial EM for this technology is proposed (**Figure 12**).

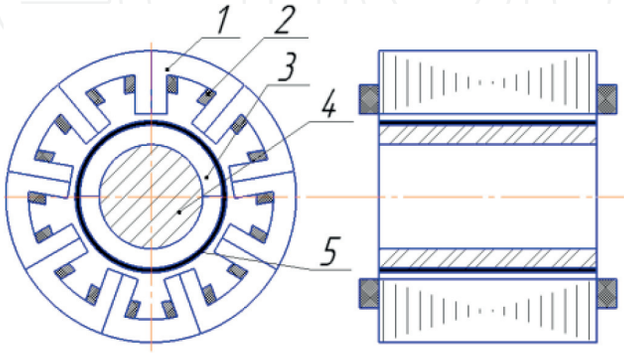

Figure 7. EM with a tooth-coil winding and a stator magnetic core made of AMM: 1 is a stator magnetic core; 2 is a tooth-coil winding; 3 is the HCPM; 4 is a shaft; and 5 is a rotor sleeve.

Figure 8. Stator magnetic core made of AMM (a) and its formation technology (b).

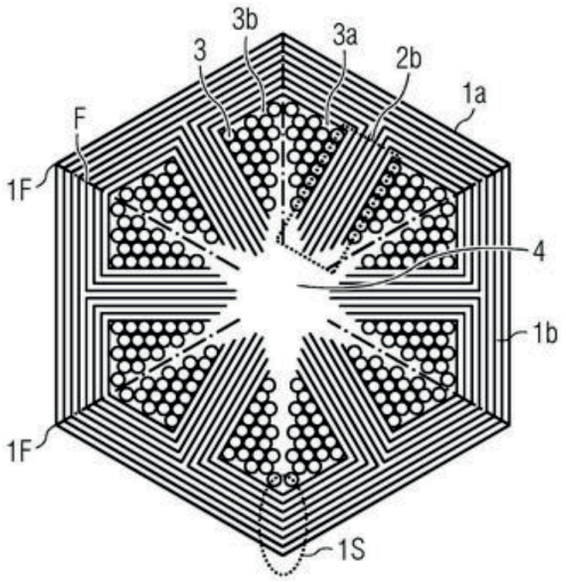

Figure 9. EM with a tooth-coil winding and a stator magnetic core made of AMM [7].

- Slotless EM with the AMM stator magnetic core. This type of AMM magnetic cores is the simplest in the manufacturing technology and has a minimum manufacturing cost. **Figure 13** shows the slotless EM designs.

Special advantages of the slotless EM are for various high-speed systems. The use of the AMM allows not only to minimize losses in the stator magnetic core but also to increase the number of poles to 8–10. This allows reducing the mass of the stator magnetic core of the slotless EM by 20–25%. In the high-speed EMs with a stator magnetic core made of electrical steel or Co-Fe alloy, the number of poles should be minimal. To reduce losses in the stator magnetic core, 2-or 4-pole EMs are used, whose stator magnetic core mass is higher than the stator magnetic core mass of multipolar EMs.

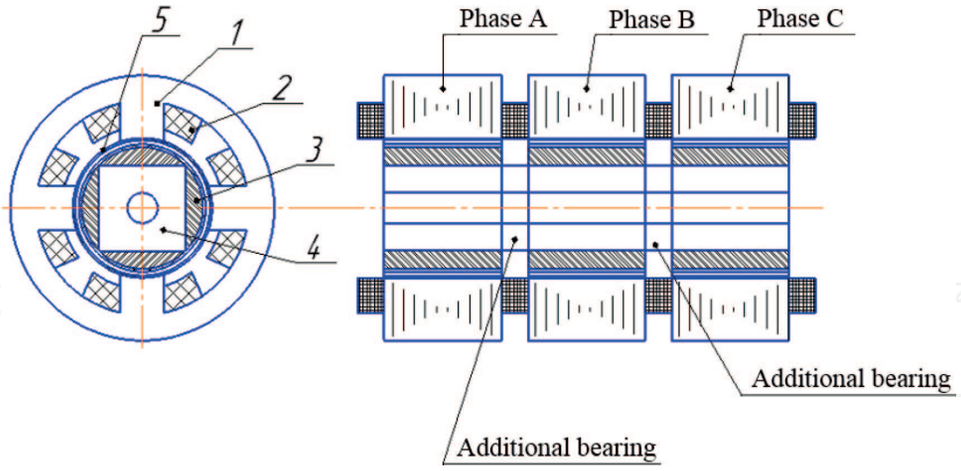

Figure 10. Sectional EM with a tooth-coil winding and a stator core made of AMM: 1 is a stator magnetic core; 2 is a tooth-coil winding; 3 is the HCPM; 4 is a shaft; and 5 is a rotor sleeve.

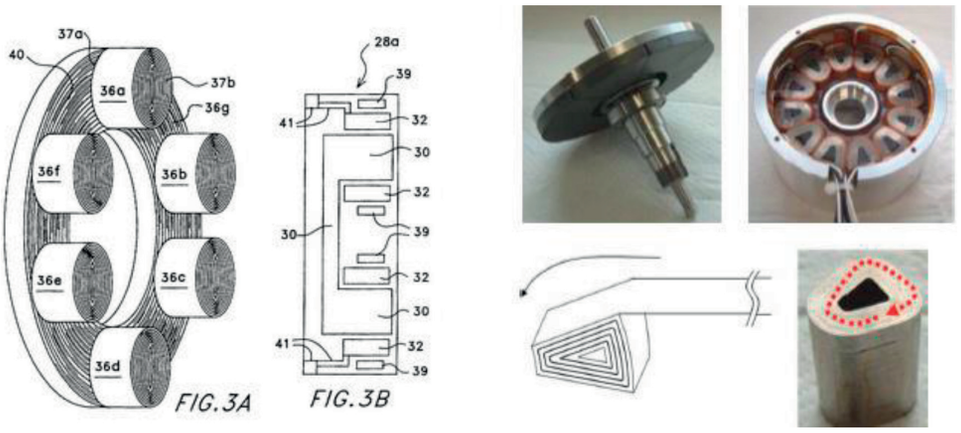

Figure 11. Prefabricated design of the AMM stator magnetic core.

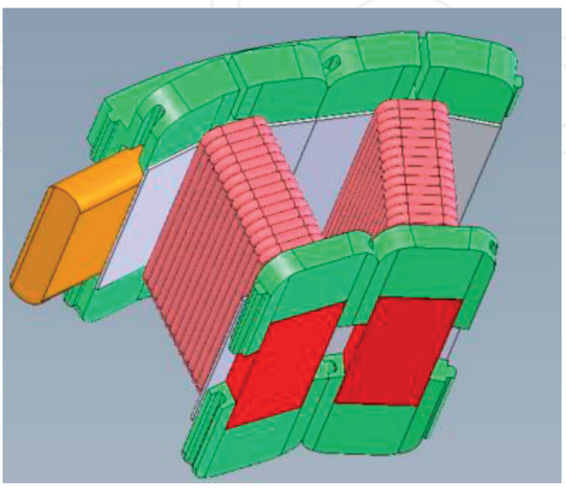

Figure 12. Assembly of the stator magnetic core made of AMM [8]

Another advantage of the slotless EM is the use of magnetic bearings in Lorentz forces, which are integrated directly into the air gap. This reduces the axial length and, thus, provides the necessary rotor dynamics and stiffness in comparison with other designs.

In addition, the slotless EM has the simple technology of producing a slotless stator magnetic core, which makes this EM class practically the only technical solution that allows the creation of ultra-high-speed micromotors and microgenerators. The slot absence results in minimization losses in the HCPM caused by tooth harmonics.

The main disadvantage of the slotless EM is that the entire winding is located in the air gap, and this leads to its significant increase. At the same time, losses to the skin effect and eddy currents in strands appear in the winding, as the entire magnetic field in the air gap crosses the winding.

The efficiency of the slotless EM with HCPM is largely determined by the number of poles, winding type, and also manufacturing method of the slotless stator magnetic core (wound or stamped). The winding type of the slotless EM with HCPM determines:

- the air gap value and energy characteristics of the slotless EM, since the entire winding is located in the air gap;
- the efficiency, which is largely determined by winding and additional losses (loss of proximity effect and eddy currents), as well as thermal loads on various EM elements;
- overall dimensions and mass of the slotless EM: mass and size parameters of the slotless EM depend on the end winding axial protrusion length and its mass);
- working capacity of the slotless EM under load and overload: the structural scheme of the winding determines the scattering resistance (xs) and accordingly the magnitude of the armature reaction demagnetizing field;
- a structural diagram of the power electronics used in conjunction with the slotless EM; the harmonic composition of the voltage determines the size of the filters and depends on the winding type).

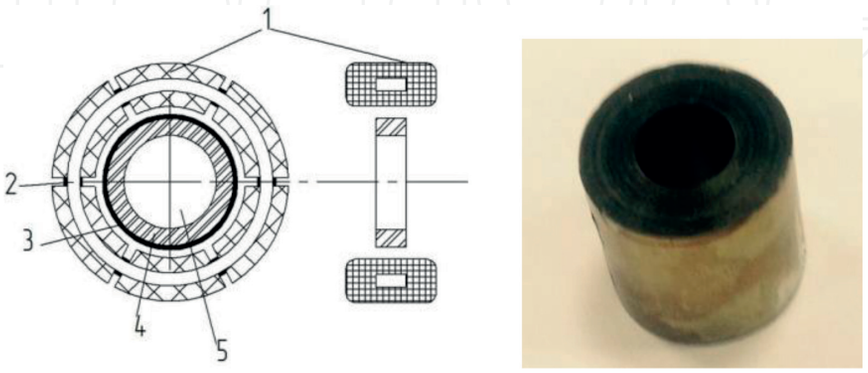

Figure 13. The slotless EM with the AMM stator magnetic core: 1 is a winding; 2 is a stator magnetic core; 3 is a rotor sleeve; 4 is the HCPM; and 5 is a shaft.

The manufacturing technology of the stator magnetic core determines:

- stator magnetic core losses; and
- the technological complexity of its manufacture, as well as the mass and size parameters of the slotless EM, which are determined by the fill factor of the stator magnetic core.

Thus, all the main parameters, which characterize the efficiency of the slotless EM, depend on the winding type, number of poles and stator magnetic core design. Therefore, the selection of these elements should be made with particular accuracy.

Typically, either a distributed winding or a toroidal winding is used in the slotless EM. Each of these windings has its disadvantages. The distributed winding is characterized by technological complexity of manufacturing, and the toroidal winding provides higher losses in copper due to the inability to use half of the winding. The possibility of using a tooth-coil winding in the slotless EM, and also a comparison of the effectiveness of a tooth-coil winding and a toroidal one in a two-pole and 10-poles slotless EM is considered in this work.

Two-pole slotless EM with a tooth-coil winding and its connection scheme is presented in **Figure 14a** and **b** accordingly. Ten-pole slotless EM with a toroidal winding and its connection scheme is presented in **Figure 14c** and **d** accordingly.

The tooth-coil winding allows achieving a minimum end winding axial protrusion length, and its manufacturing technology is simpler than the toroidal winding. At the same time, due to the MMF spatial harmonic, the tooth-coil winding should have a distorted voltage shape, which will lead to additional losses in the HCPM.

To evaluate the effectiveness of the design, four experimental slotless EMs were designed and manufactured: a 2-pole and a 10-pole slotless EMs with a HCPM and a toroidal winding, and a 2-pole and a 10-pole slotless EMs with a HCPM and a tooth-coil winding (**Figure 15**). To simplify the laboratory studies, the experimental models were performed with a low power for a reduced rotational speed of 3000 rpm, which also simplifies the requirements for bearings. The stator magnetic core of prototypes was low saturated. Thus, four stators and two rotors were made.

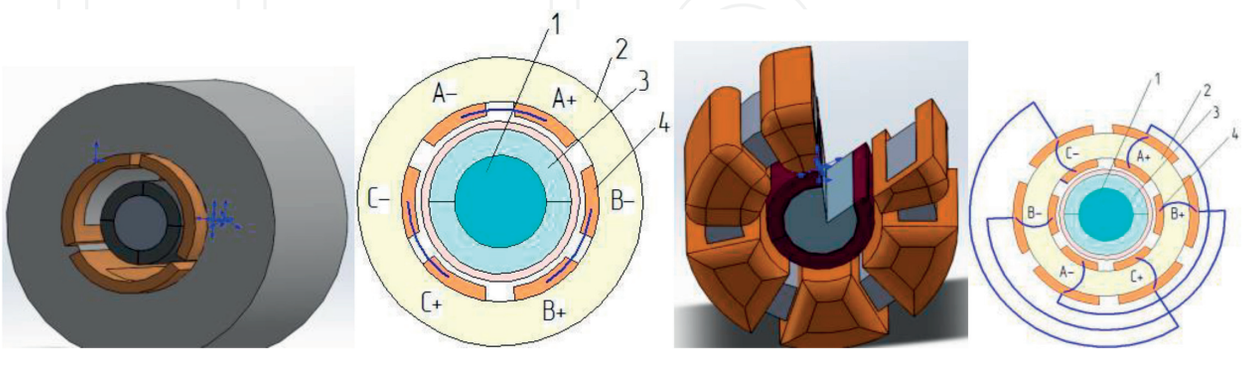

Figure 14. Slotless EM with a concentrated winding (a) and its connection scheme (b) and slotless EM with a toroidal winding (c) and its connection scheme (d): 1 is a rotor core; 2 is a slotless stator magnetic core; 3 is the HCPM; and 4 is a winding.

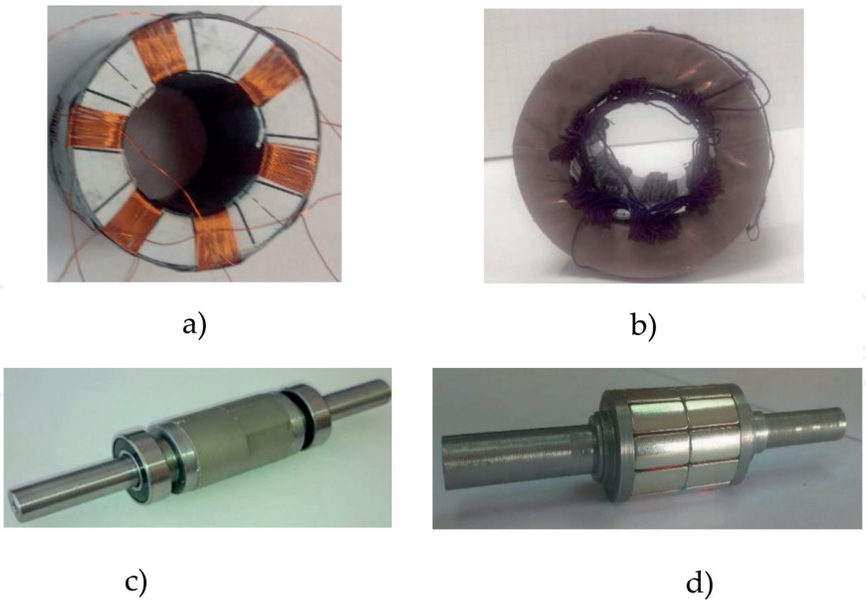

Figure 15. (a) The stator core with toroidal winding; (b) the stator core with concentrated winding; (c) 2-pole rotor; and (d) multi-pole rotor.

Analysis of various winding types of slotless EMs with HCPM can be made using only computer simulation methods, but at the same time, it does not allow to assess the technological manufacturing complexity. From the known works, it can be concluded that the main operating mode of the slotless EM with HCPM is the generator mode. One of the main characteristics of the generator mode for aerospace EMs is the voltage dependence on the load current, which is determined by the inductive resistance of the winding. According to the experimental results, four models and four computer models were developed in the Ansys Maxwell software package, and the simulation and experimental results are compared.

Therefore, the procedure for the design selection was as follows:

1. Design calculation and creation of experimental prototypes and its research under load in the generator mode. An external characteristic, oscillograms of current and voltage, harmonic composition of current and voltage, and estimation of the winding losses are obtained.
2. Creation of a computer model in the Ansys Maxwell software package. The discrepancy between the experimental and computer simulation data should not exceed 5%. At this stage, the magnetic field distribution patterns are obtained for each considered slotless EM, and losses in permanent magnets are estimated.
3. Experimental studies of losses in a stator core made of AMM at different frequencies.
4. Selection of topology. According to the experimental and computer results obtained, different topologies of slotless EMs with HCPM are evaluated.

As a research result, it was established that the two-pole slotless EM with a tooth-coil winding has the less steep external characteristic and the voltage decreasing is below

10–15% at a load. The steepest external characteristic is in 10-pole slotless EM with a tooth-coil winding. The open circuit voltage is different from the voltage at one-and-a half overload by 210%. This is explained by the fact that with increasing number of poles, the inductive scattering resistance increases significantly; thus, the multi-pole slotless EM with HCPM is essentially a high-reactance permanent magnet EM. This EM type is most applicable in aerospace engineering, since it provides the most reliable short-circuit protection of the slotless EM and the system in which it is installed. Thus, from the analysis of the experimental external characteristics, it can be concluded that the 10-pole slotless EM with a HCPM and a tooth-coil is most effective.

4.3. Soft magnetic composite materials (Somaloy)

Somaloy is a soft magnetic composites produced by Höganäs in the powder form for sintering and pressing. The advantage of these materials is the nonwaste-producing technology. The technological process of producing magnetic cores has a certain complexity. **Figure 16** shows the magnetization curves for 1P Somaloy 500P and 1P Somaloy 700P. **Table 3** presents characteristics of different soft magnetic composite materials. It can be seen that soft magnetic composite materials have significant specific losses, which limits their use in high-speed EMs. Due to the high adaptability of this material, it can find wide application in the EM with low rotational speeds.

4.4. Ironless stator magnetic cores

The ironless stator magnetic cores are magnetic cores made of nonmagnetic nonconductive materials. The ironless stator magnetic cores are used in superconducting EMs when significant magnetic flux density in the air gap leads to a supersaturation of the magnetic core. In addition, the ironless stator magnetic cores can find application in ultra-high-speed EMs with rotational speed above 1,000,000 rpm.

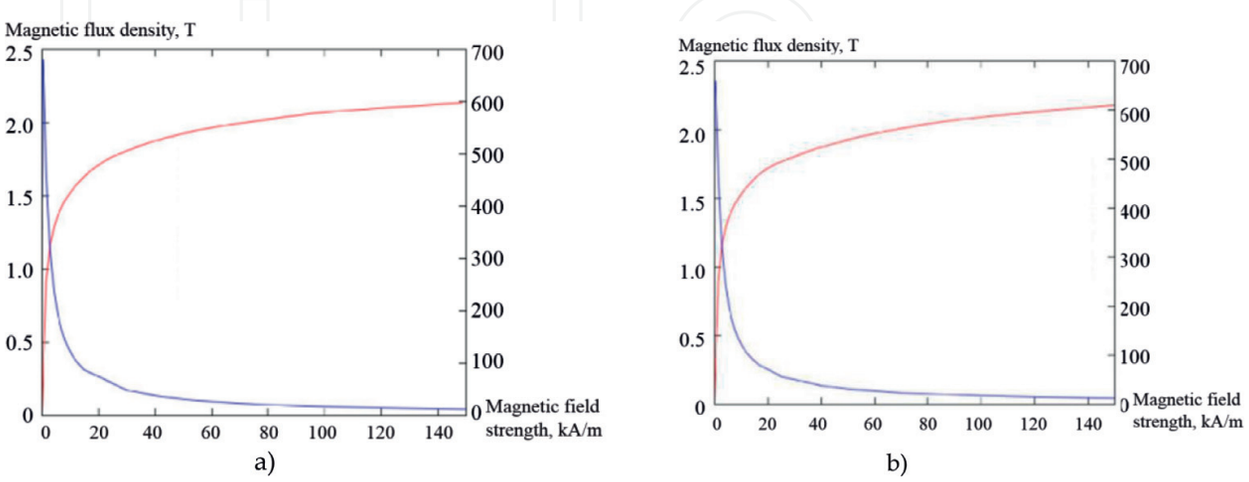

Figure 16. The magnetization curves for 1P Somaloy 500P (a) and 1P Somaloy 700P (b).

Material type	Magnetic flux density at a magnetic field strength of 10,000 A/m (T)	Specific losses (W/kg)			
		5 × 5 mm			15 × 15 mm
		100 Hz	400 Hz	1000 Hz	1000 Hz
1PSomaloy 130i	1.4	12	54	145	147
1PSomaloy 700	1.56	10	44	131	158
1PSomaloy 700 HR	1.53	10	46	134	145
3PSomaloy 700	1.61	10	46	137	189
3PSomaloy 700 HR	1.57	11	48	137	157
3P Somaloy 1000	1.63	10	46	144	287
5PSomaloy 700 HR	1.57	6	32	104	115

Table 3. Characteristics of different soft magnetic composite materials.

5. Permanent magnet types

To select permanent magnets of high-speed EMs, the demagnetization curve of permanent magnets at different temperatures (**Figures 17** and **18**), residual magnetic flux density (Br), coercive force by magnetic flux density (HcB) and magnetization (Hcj), maximum operating temperature, Curie temperature, temperature coefficients by magnetic flux density and coercive force were used.

5.1. Temperature coefficients by magnetic flux density and coercive force

Under the temperature influence, the coercive force and the residual magnetic flux density of the permanent magnets decrease (**Figure 18**). It is analytically determined as follows:

$$B_r(\Theta) = B_r\left(1 - \frac{k_{Br}(\Theta_{BПM} - 20)}{100}\right), \tag{14}$$

$$H_c(\Theta) = H_c\left(1 - \frac{k_{Hc}(\Theta_{BПM} - 20)}{100}\right), \tag{15}$$

where $B_r(\Theta)$, $H_C(\Theta)$ are, respectively, the values of the magnetic flux density and coercive force of the HCPM; B_r, H_C are, respectively, the values of the residual magnetic flux density and coercive force of the HCPM, indicated in the technical characteristics; $\Theta_{BПM}$ is the HCPM temperature; kBr is a temperature coefficient by residual magnetic flux density; and kHc is a temperature coefficient by coercive force.

In Eqs. (20) and (21), temperature coefficients are used constant, while the temperature coefficients of the HCPM are constant only at temperatures below 100–120°C. At higher temperatures,

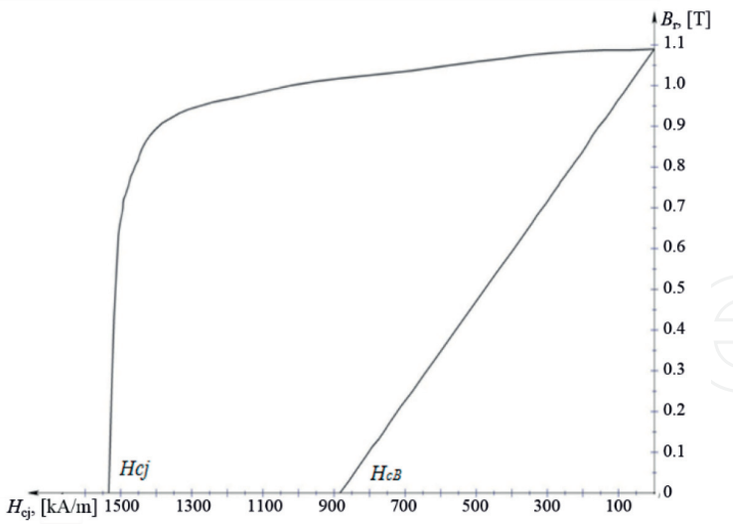

Figure 17. The demagnetization curve of Sm_2Co_{17} permanent magnets.

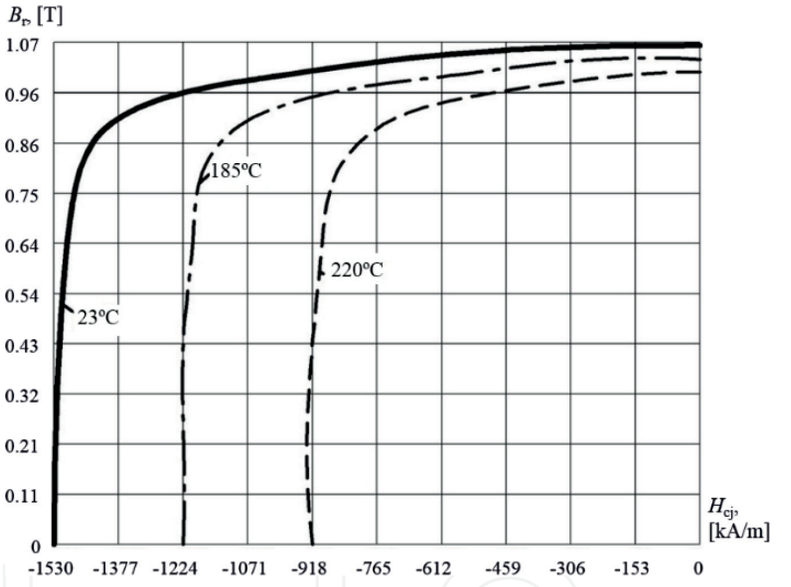

Figure 18. The demagnetization curve of Sm_2Co_{17} at different temperatures.

coefficients vary with temperature. Thus, the temperature characteristic of the HCPM demagnetization is nonlinear at temperatures above 100–120°C.

In modern high-speed EMs, several HCPM types are used: SmCo, SmCoFeCuZr, and NdFeB alloys. The main advantage of the HCPM based on SmCo and SmCoFeCuZr is their high temperature stability as well as corrosion resistance compared to NDFeB. The SmCo Curie temperature is above 800°C; the temperature coefficients by induction and coercive force are −0.04 and −0.3, respectively. The Curie temperature of NdFeB is above 300°C, and temperature coefficients by induction and coercive force are −0.11 and −0.6, respectively. NdFeBs have higher energy characteristics than SmCo by 20–30%. Nevertheless, their low temperature stability does not allow the efficient use of these high-energy characteristics. **Figure 19** shows

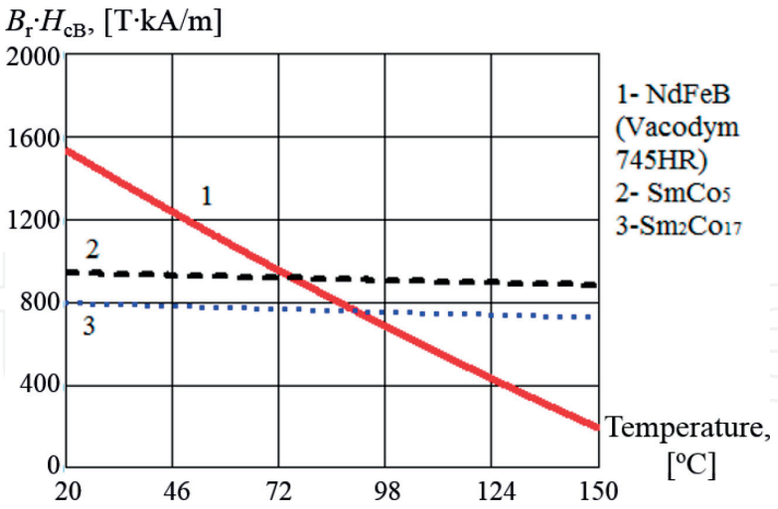

Figure 19. Characteristic dependences of SmCo, SmCoFeCuZr, and NdFeB at various temperatures.

the characteristic dependences of SmCo, SmCoFeCuZr, and NdFeB at various temperatures. For comparison, the most energetically powerful NdFeB sample Vacodym 745 HR with Br = 1.44 T, HcB = 1065 kA/m were selected. Dependencies are constructed for a product $B_r \cdot H_{cB}$. It was found that the use of NdFeB is expedient at temperatures of the HCPM below 60–70°C. **Table 4** presents properties of the SmCo and NdFeB.

In addition, the high-temperature HCPMs based on SmCoFeCuZr alloys with operation temperatures up to 700°C (T 500 and T 550) have been developed.

In the HCPM manufacture, resin-bonded magnet and rubber ferrite are often used. They have higher temperature coefficients than ordinary magnets and have mechanical properties similar to plastics, but their energy characteristics are lower than the ceramic or metal HCPM obtained by sintering.

Property	**NdFeB**	**$SmCo_5$**	**Sm_2Co_{17}**
Density (g/cm^3)	7.4	8.3	8.4
Young's modulus (GPa)	150	—	—
Cross-breaking strength (MPa)	210–290	180	150
Rupture strength (MPa)	70–130	40	35
Vickers hardness (HV)	600	450–500	500–600
Electrical resistance (Ohm/m)	$1.6 \cdot 10^{-6}$	$5 \cdot 10^{-7}$	$8.6 \cdot 10^{-7}$
Specific heat (J/kg · K)	440	370	340–390
Thermal conductivity (W/m · K)	9	12	13
The temperature coefficient of linear expansion along the magnetization direction (10^{-6}/K)	5	6	8
Temperature coefficient of linear expansion across the magnetization direction (10^{-6}/K)	−1	13	11

Table 4. Mechanical, electrical, and thermal of the SmCo and NdFeB.

5.2. Climate testing and long-term storage of various HCPM types

Results of corrosion and climate tests of Sm_2Co_{17}, $SmCo_5$, and NdFeB are presented in [9]. It is shown that Sm-Co alloys are susceptible to corrosion both during storage and in a heated storage room, but their magnetic properties change insignificantly (~ 1–2%). The greatest changes both in magnetic properties and in corrosion occur in the first storage year, and SmCo5 alloys are more resistant to long-term storage than Sm_2Co_{17} alloys. In addition, NdFeB is significantly susceptible to corrosion and practically has not been tested for long-term storage.

5.3. Radiation resistance of HCPM

For EM with HCPM for special areas of industry, including the space and nuclear industries, an important criterion in the HCPM selection is their resistance to radiation exposure. In [10], studies of the radiation resistance of Sm_2Co_{17}, $SmCo_5$, and NdFeB are presented. It was established that the radiation resistance of the SmCo is above 1018 neutrons/cm^2 and the radiation resistance of the NdFeB is lower. The magnetic property loss of NdFeB in radiation irradiation is in most cases caused not by the weak stability of NdFeB to neutron radiation but by their radiation heating. Therefore, it is not recommended to use NdFeB in EMs, which can be exposed to significant radiation exposure.

6. Conclusion

In this chapter, materials used in high-speed EMs with HCPM are presented. The application areas of high-speed EMs are shown. Practical recommendations for the selection of active and structural components of high-speed EMs are given. The mechanical strength calculation of the rotor sleeve is shown. The obtained results can be used in practice in the EM design and in the further research.

Author details

Flyur R. Ismagilov, Viacheslav Ye. Vavilov* and Valentina V. Ayguzina

*Address all correspondence to: s2_88@mail.ru

Ufa State Aviation Technical University, Ufa, Russia

References

[1] Dr. Ralph Funck Composite Materials in High Efficient Sleeve Applications of Electric Machines [Internet]. Available from: http://www.circomp.de/de/downloads/CirComp-high-efficient-sleeveapplications.pdf [Accessed: March 28, 2018]

[2] Kruchinina IY, Antipov VI. Problematic issues of creation high-speed mini-turbogenerators and ways of their decision (in Russian). Management Information Systems. 2012;**4**:25-34

[3] Ledovsky AN. Electrical Machines with High-coercive Permanent Magnets (in Russian). Vol. 169. Moscow: Energoatomizdat; 1985

[4] Golovanov DV, Kovarsky ME, Magin VV, Trunov IG. Methods of calculation of high-speed generators for gas-turbines. Questions of Electromechanics, 2012;**126**:3-8

[5] Tao Z, Ye X, Huiping Z, Hongyun J. Strength design on permanent magnet rotor in high speed motor using finite element method. Telkomnika Indonesian Journal of Electrical Engineering. 2014;**12**(3):1758-1763

[6] Zwyssig C, Kolar JW, Round SD. Mega-speed drive systems: Pushing beyond 1 million RPM. IEEE/ASME Transactions on Mechatronics. 2009;**14**(5):564-574

[7] Borisavljevic A, Polinder H, Ferreira JA. Enclosure design for a high-speed permanent magnet rotor. Power Electronics, Machines and Drives (PEMD);**2**:817-822

[8] McPherson MW, Hirzel AD. Stator used in an electrical motor or generator with low loss magnetic material and method of manufacturing a stator. Patent US2013278103

[9] Tyutnev AP, Sergeyev VV, Semyonov VT, Stanolevich GP. To a question of radiation firmness of permanent magnets on the basis of rare-earth elements (in Russian). Electromechanics Questions. 2013;**133**(2):18-27. VNIIEM

[10] Stanolevich GP, Fedoseev NV, Timakov SA, Borisov SL. Stability of rare-earth SmCo magnets to long storage (in Russian). Electromechanics Questions. 2014;**139**(2):29-34. VNIIEM

IntechOpen